Electronic Supplementary Material (ESI) for CrystEngComm.

A Novel Copper(I) Metal-Organic Framework as a Highly Efficient and Ultrasensitive Electrochemical Platform for Detection of Hg(II) Ion in Aqueous Solution

Xiao-Qing Wang[a]*, Jing Tang[a], Xuehui Ma[a], Dan Wu[a] and Jie Yang[b]

[a] *Department of Chemistry, College of Science, North University of China, Taiyuan 030051, PR China*

[b] *Shandong Provincial Key Laboratory of Chemical Energy Storage and Novel Cell Technology, and School of Chemistry and Chemical Engineering, Liaocheng University, Liaocheng 252000, PR China*

Table S1 Selected bond lengths (Å) and angles (°) of complex **1**.

Cu1—Cu1^{i}	2.801(4)	Cu1—Cl1	2.441(3)
Cu1—Cl1^{i}	2.441(3)	Cu1—N1^{ii}	1.977(7)
Cu1—N1	1.977(7)	Cu1—Cl3^{iii}	2.437(3)
Cu1—Cl3	2.437(3)	Cu3—N6	1.985(9)
Cu3—N5	1.986(9)	Cu2—Cl2^{iv}	2.435(3)
Cu2—Cl2	2.435(3)	Cu2—N3	1.953(7)
Cu2—N3^{iv}	1.953(7)	Cu4—Cu4^{v}	2.778(9)
Cu4—Cl4	2.458(7)	Cu4—Cl4^{v}	2.425(7)
Cu4—N8	2.054(14)	Cl1^{i}—Cu1— Cu1^{i}	54.99(6)
Cl1—Cu1—Cu1^{i}	54.99(6)	Cl1^{i}—Cu1—Cl1	109.97(12)
N1—Cu1—Cu1^{i}	119.8(2)	N1^{ii}—Cu1—Cu1^{i}	119.8(2)
N1^{ii}—Cu1—Cl1^{i}	106.54(13)	N1—Cu1—Cl1	106.54(13)
N1—Cu1—Cl1^{i}	106.54(13)	N1^{ii}—Cu1—Cl1	106.54(13)
N1^{ii}—Cu1—N1	120.5(5)	Cl3—Cu3—Cl3^{iii}	94.02(12)
N6—Cu3—Cl3^{iii}	108.19(18)	N6—Cu3—Cl3	108.19(18)
N5—Cu3—Cl3^{iii}	110.35(19)	N5—Cu3—Cl3	110.35(19)

N5—Cu3—N6	122.1(4)	Cl2^{iv}—Cu2—Cl2	93.58(13)
N3—Cu2—Cl2^{iv}	109.04(2)	N3^{iv}—Cu2—Cl2	109.04(2)
N3—Cu2—Cl2	111.05(19)	N3^{iv}—Cu2—Cl2^{iv}	111.05(19)
N3—Cu2—N3^{iv}	120.0(5)	Cl4—Cu4—Cu4^{v}	57.44(18)
Cl4^{v}—Cu4—Cu4^{v}	55.88(18)	Cl4^{v}—Cu4—Cl4	110.6(2)
N8—Cu4—Cu4^{v}	120.4(5)	N8—Cu4—Cl4^{v}	106.4(4)
N8—Cu4—Cl4	107.0(4)	Cu4^{v}—Cl4—Cu4	69.3(2)
Cu1—Cl1—Cu1^{i}	70.03(12)	Cu3—Cl3—Cu3^{vi}	85.89(12)
Cu2^{vii}—Cl2—Cu2	86.42(13)	C14—N8—Cu4	124.0(10)
C12—N6—Cu3	131.9(8)	C10—N6—Cu3	123.7(8)
C16—N3—Cu2	130.0(7)	C5—N3—Cu2	124.6(6)
C9—N5—Cu3	129.5(9)	C8—N5—Cu3	127.1(9)
C1^{vi}—N1—Cu1	121.9(4)	C1—N1—Cu1	121.9(4)

Symmetry codes: (i) 1-x,-y,-z; (ii) +x,-y,-z; (iii) 1-x,+y,+z; (iv) 1/2-x,1/2-y,+z; (v) 3/2-x,-y,1/2-z; (vi) +x, +y,-z.

Table S2 Bond valence sum calculations for Cu ions based on the crystal data in complex **1**.

central ion	Bond type	r_{ij}/Å	S_{ij}	V_{ij}
Cu1	Cu1-Cl1	2.441	0.3028	1.096
	Cu1—Cl1^{i}	2.441	0.3028	
	Cu1—N1	1.977	0.4899	
	Cu1—N1^{ii}	1.977	0.4899	
Cu2	Cu2—Cl2	2.435	0.3078	1.138
	Cu2—Cl2^{iv}	2.435	0.3078	
	Cu2—N3	1.953	0.5227	
	Cu2—N3^{iv}	1.953	0.5227	
Cu3	Cu3—Cl3	2.437	0.3061	1.092
	Cu3—Cl3^{iii}	2.437	0.3061	
	Cu3—N6	1.985	0.4794	
	Cu3—N5	1.986	0.4794	
Cu4	Cu4—Cl4	2.458	0.2892	1.003

	Cu4—Cl4[v]	2.425	0.3162
	Cu4—N8	2.054	0.3979
	Cu4—N8[v]	2.054	0.3979

Symmetry codes: (i) 1-x,-y,-z; (ii) +x,-y,-z; (iii) 1-x,+y,+z; (iv) 1/2-x,1/2-y,+z; (v) 3/2-x,-y,1/2-z; (vi) +x, +y,-z.

Table S3. Comparison of reported MOF-based sensors for Hg(II) detection.

	MOF	Methods	Linear Range	Detection Limit	Ref.
1	AB/Cu_3Cl_3(bimpy)$_3$/GCE	ESC	2 μM – 64 μM	1.1 nM	This work
2	$NiCo_2O_4$ nanoplatelets/GCE		0.8 - 2.0 μM	42.9 nM	28a
3	$MnFe_2O_4$@Cys/GCE		1.4 - 3.0 μM	208 nM	28b
4	GA-UiO-66-NH_2/GCE		0.005 -3.0 μM	2 nM	13
5	3 D (Co, Mn)$_3O_4$/Ni composite foam		0.5 - 4.0 μM	13 nM	28c
6	Cu-MOFs		10 fM - 100 nM	4.8 fM	24a
7	ssDNA/Au electrode		0.1 - 2.0 μM	100 nM	29a
8	Gold ultramicroelectrode arrays		0.01 - 1.0 μM	16 nM	29b
10	Fe_3O_4 -chitosan/GCE		0.4 - 1.1 μM	95.7 nM	29c
11	$NiCo_2O_4$/Ni foam		0.8 - 2.8 μM	9.91 nM	29d
12	PCN-221	FL	50 - 1000 μM	0.12 μM	30a
13	$[Pb_2(2\text{-NCP})_2(L_1)]_n$		0 - 1.0 mM	10^{-7} M	30b
14	$\{[Co_2(L)(hfpd)(H_2O)]\cdot 1.75H_2O\}_n$		0 - 200 μM	4 μM	30c
15	$[Co(NPDC)(bpee)]\cdot DMF\cdot 2H_2O$		0 - 120 μM	4.1 μM	30d
16	$[Zn(H_4L)(2,2'\text{-biim})]$		0 - 25 μM	0.53 μM	31a
17	$\{[Tb_2(bpda)_3(H_2O)_3]\cdot H_2O\}_n$		0 - 10^{-3} M	7.2 nM	31b
18	$\{[Mn_2(Bript)_2(4,4'\text{-bpy})_{.5}(DMF)]\cdot(H_2O)\}_n$		0 - 0.3 M	48 μM	31c
19	UiO-66-PSM		0 - 78.1 μM	5.88 μM	31d
20	ZnAPA		0 - 400 μM	0.1243 μM	31e

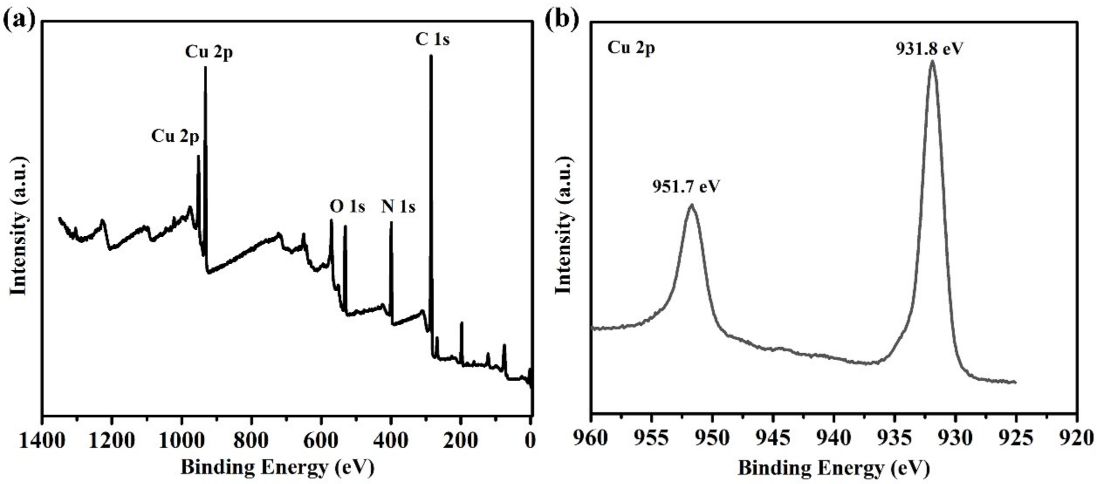

Fig. S1 (a) XPS spectra of complex **1**; (b) XPS spectra of Cu 2p of complex **1**.

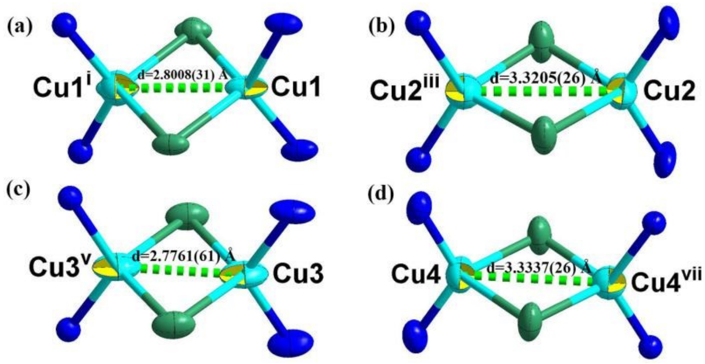

Fig. S2 The SBUs in complex **1**.

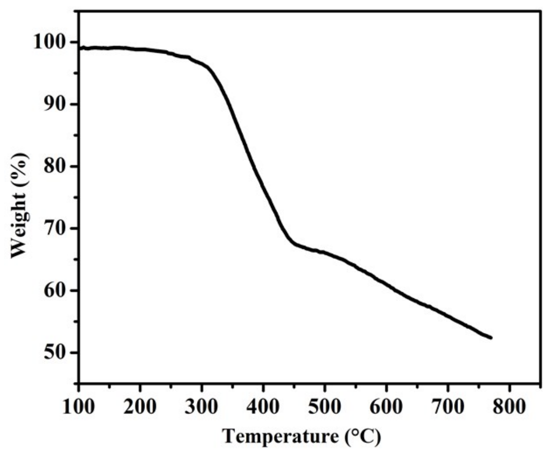

Fig. S3 TGA pattern of complex **1.**

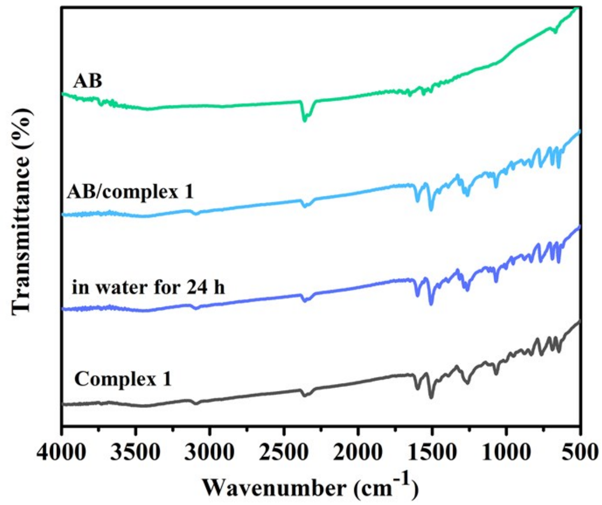

Fig. S4 FTIR spectra of complex **1**, **1** after soaking in water for 24 h, AB and AB/complex **1**.

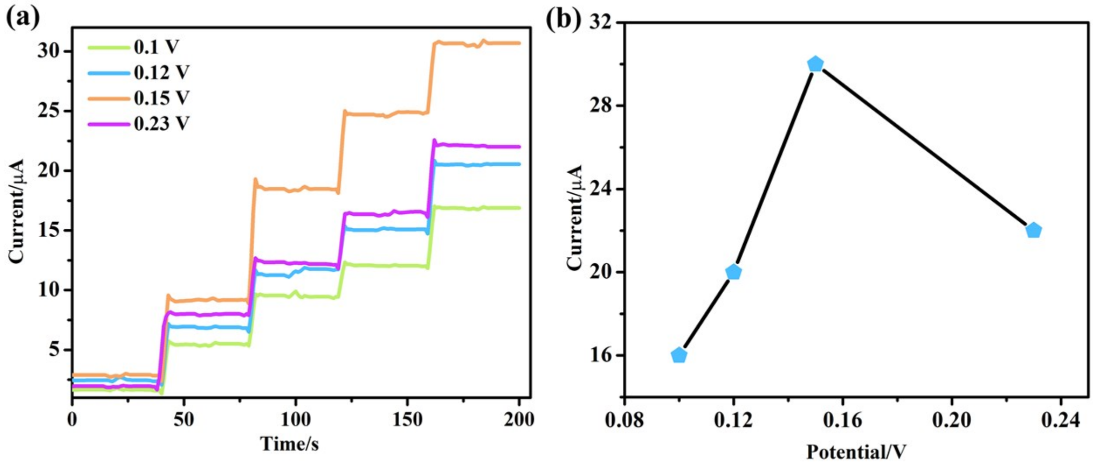

Fig. S5 (a) Chronoamperometric responses of AB/Complex **1**/GCE at different potential (0.1, 0.12, 0.15, 0.23 V) with addition of 50 μL Hg^{2+} in 0.1 M PBS solution, (b) The current intensity *vs.* potential.

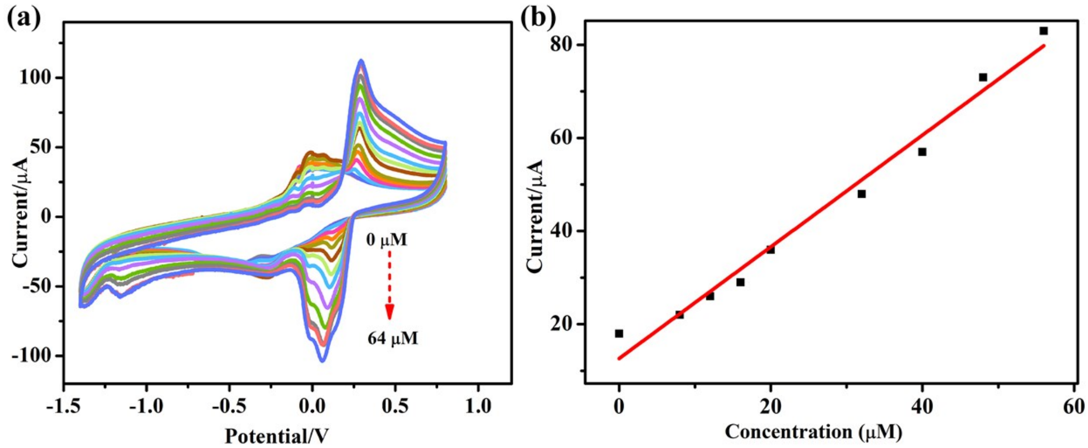

Fig. S6 (a) CV responses of AB/complex **1**/GCE upon successive addition of Hg^{2+} over a concentration range of 0 μM to 64 μM in PBS solution; (b) The corresponding calibration plot of current *vs.* the concentrations of Hg^{2+}.

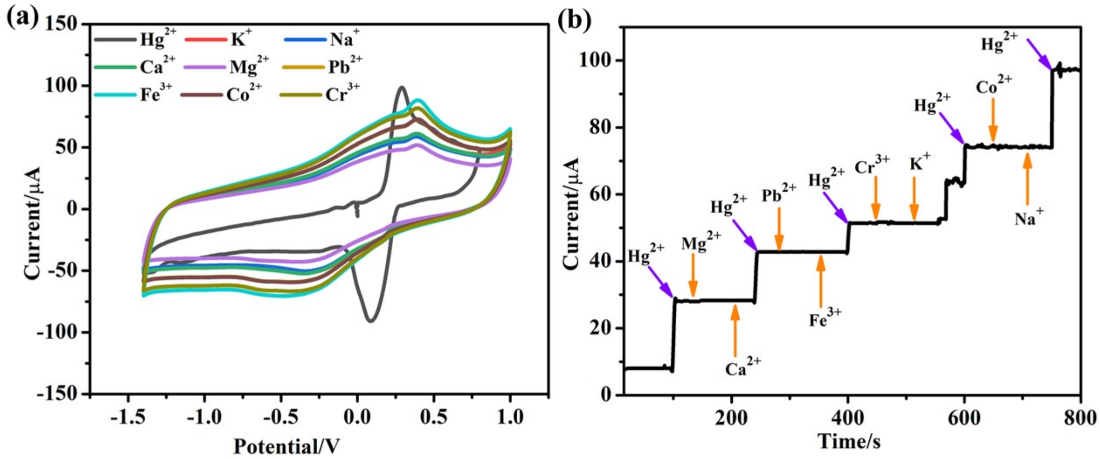

Fig. S7 (a) CV curves of other metal ions for AB/complex **1**/GCE; (b) The specificity of the sensor toward Hg^{2+} against different metal ions (the concentration of each interfering ion is 0.01 M).

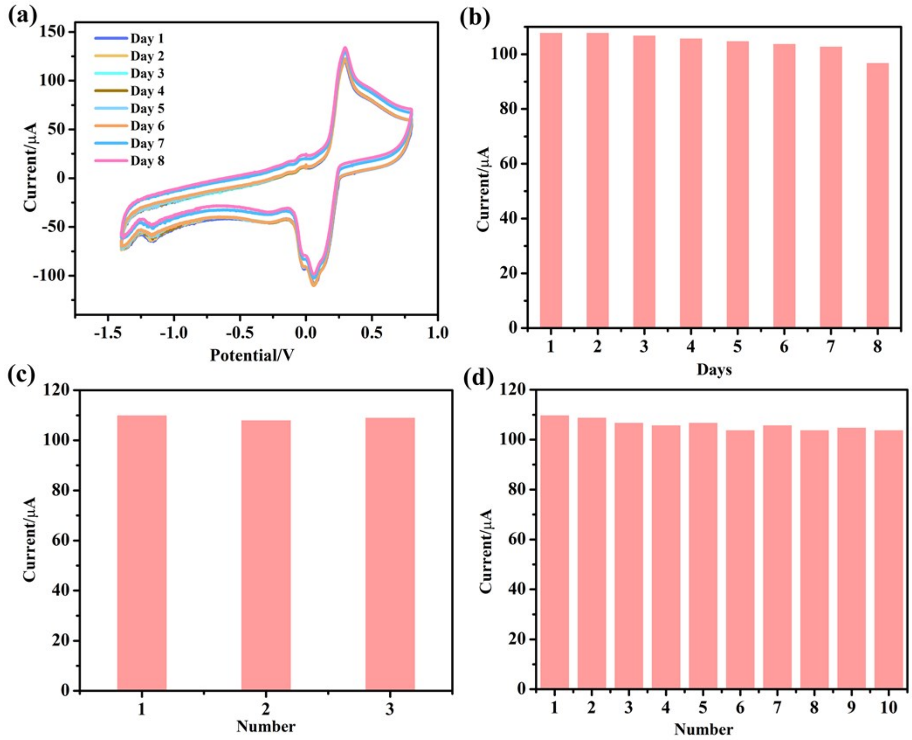

Fig. S8 (a) The CV response on the sensor for 0.064 mM Hg^{2+} analysis after eight days; (b) The current intensity after eight days; (c) The current responses of three different AB/complex **1**/GCE sensors at the same condition in 0.1 M PBS containing 0.064 mM Hg^{2+};(d) The current responses of the same AB/complex **1**/GCE sensor for ten replicate experiments in 0.1 M PBS containing 0.064 mM Hg^{2+}.